

## A B-cell receptor-related gene signature predicts response to ibrutinib treatment in mantle cell lymphoma cell lines

Mantle cell lymphoma (MCL) is a B-cell malignancy with a broad range of clinical and biological features. Once all MCL patients were considered to have a poor prognosis. However, it is now fully established that a group of MCL patients may experience an indolent disease without needing treatment for years.<sup>1-6</sup> Even among patients requiring treatment, prognosis is highly heterogeneous, with some patients experiencing prolonged remissions and others suffering rapid relapse. For this reason, there is a critical need for reproducible biomarkers that can be incorporated into clinical trial design and ultimately used to guide clinical decisions.

We have recently developed a survival predictive model for patients with advanced MCL aged <65 years, treated with an intensified induction chemo-immunotherapy followed by high-dose chemotherapy and autologous stem cell transplantation, in the context of the "Fondazione Italiana Linfomi" (FIL) MCL-0208

phase III randomized clinical trial.<sup>7</sup> This model is: 1) based on the quantitative real-time polymerase chain reaction (qRT-PCR) values of six representative gene reaction (qRT-PCR) values of six representative genes (*AKT3*, *BCL2*, *BTK*, *CD79B*, *PIK3CD*, and *SYK*); 2) is applicable both to peripheral blood (PB) MCL cells and to formalin-fixed paraffin-embedded tissue specimens. It proved to be an independent predictor of short progression-free survival (PFS) along with the combined Mantle Cell Lymphoma International Prognostic Index (MIPI-c) score. Notably, this 6-gene BCR-related signature was able to identify a MCL subset with shorter PFS intervals also in the context of an external independent MCL cohort,<sup>7</sup> again treated with an intensified chemo-immunotherapy regimen.

Here we analyzed the expression levels of the six genes of the signature in a number of well-established MCL cell line models (Rec-1, Jeko-1, Mino, JVM-2, Granta-519, and Z-138) all bearing the t(11;14)<sup>8</sup> by a qRT-PCR approach identical to that previously reported.<sup>7</sup> A hierarchical clustering using these values was able to discriminate between two different groups of MCL cell lines respectively characterized by a low or high expression of

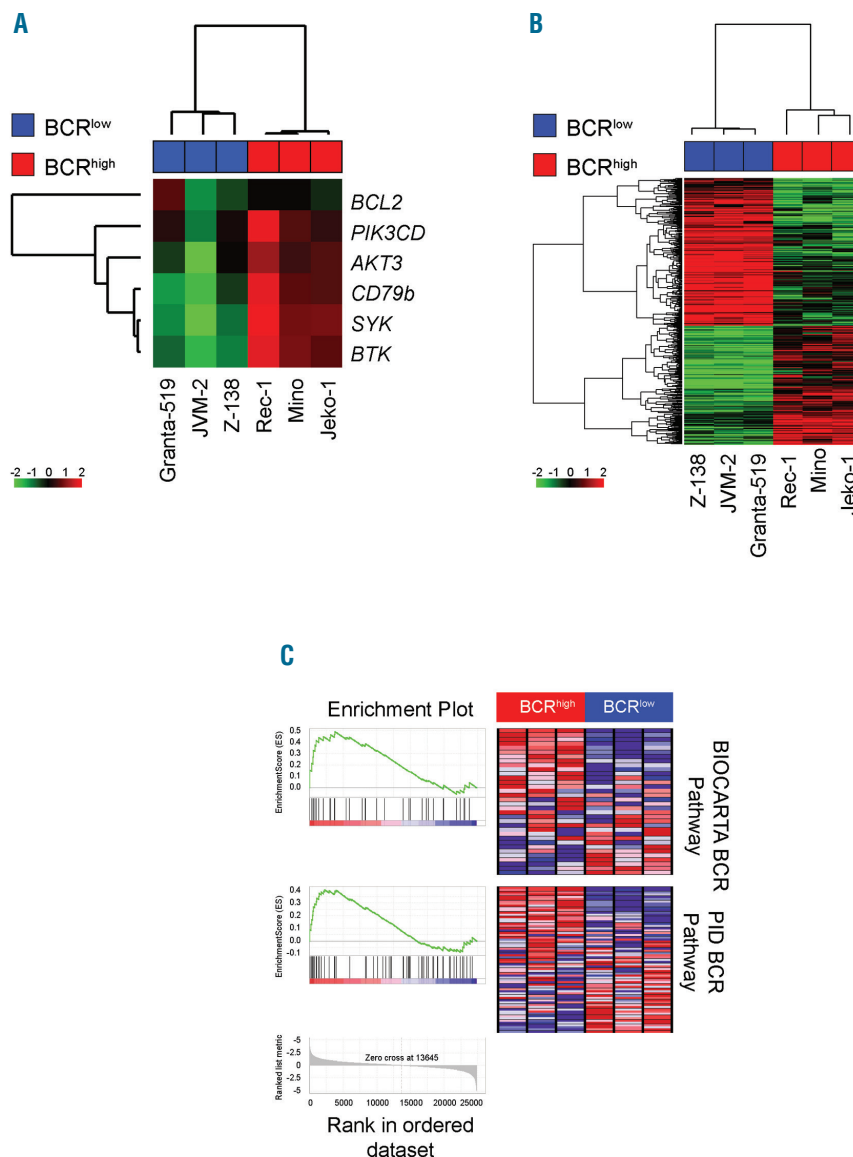


**Figure 1. Mantle cell lymphoma (MCL) cell lines and BCR categories.** (A) Quantitative real-time polymerase chain reaction (qRT-PCR) analysis of 6-gene signature in MCL cell lines. Hierarchical clustering of three BCR<sup>low</sup> MCL cell lines (blue bar under the horizontal dendrogram) and three BCR<sup>high</sup> MCL cell lines (red bar under the horizontal dendrogram), using the six gene values, is shown. BCR<sup>low</sup> and BCR<sup>high</sup> MCL cell lines were BCR<sup>high</sup> according to the Decision Tree (DT) prediction model. Color codes for gene expression values refer to mean centered log-ratio values. (B) Gene expression profile of MCL cell lines. Hierarchical clustering of three BCR<sup>low</sup> MCL cell lines (blue bar under the horizontal dendrogram) and three BCR<sup>high</sup> MCL cell lines (red bar under the horizontal dendrogram), using the 2,127 differentially expressed probes obtained by gene expression profiling (GEP), is shown. Color codes for gene expression values refer to mean centered log-ratio values. (C) GEP data of BCR<sup>low</sup> and BCR<sup>high</sup> MCL cell lines were tested for gene set enrichment using gene set enrichment analysis (GSEA). Reported are the gene sets found significantly differentially expressed between BCR<sup>low</sup> and BCR<sup>high</sup> MCL cell lines related to B-cell receptor (BCR) pathway. (Left) Plot of the enrichment score displaying the main pathway related to BCR pathway obtained from GSEA. (Right) Corresponding heat-maps highlighting the relative expression of the gene members belonging to the reported gene sets in BCR<sup>low</sup> (blue bar under the horizontal dendrogram) and BCR<sup>high</sup> (red bar under the horizontal dendrogram) MCL cell lines. Color codes for gene expression values refer to mean centered log-ratio values.

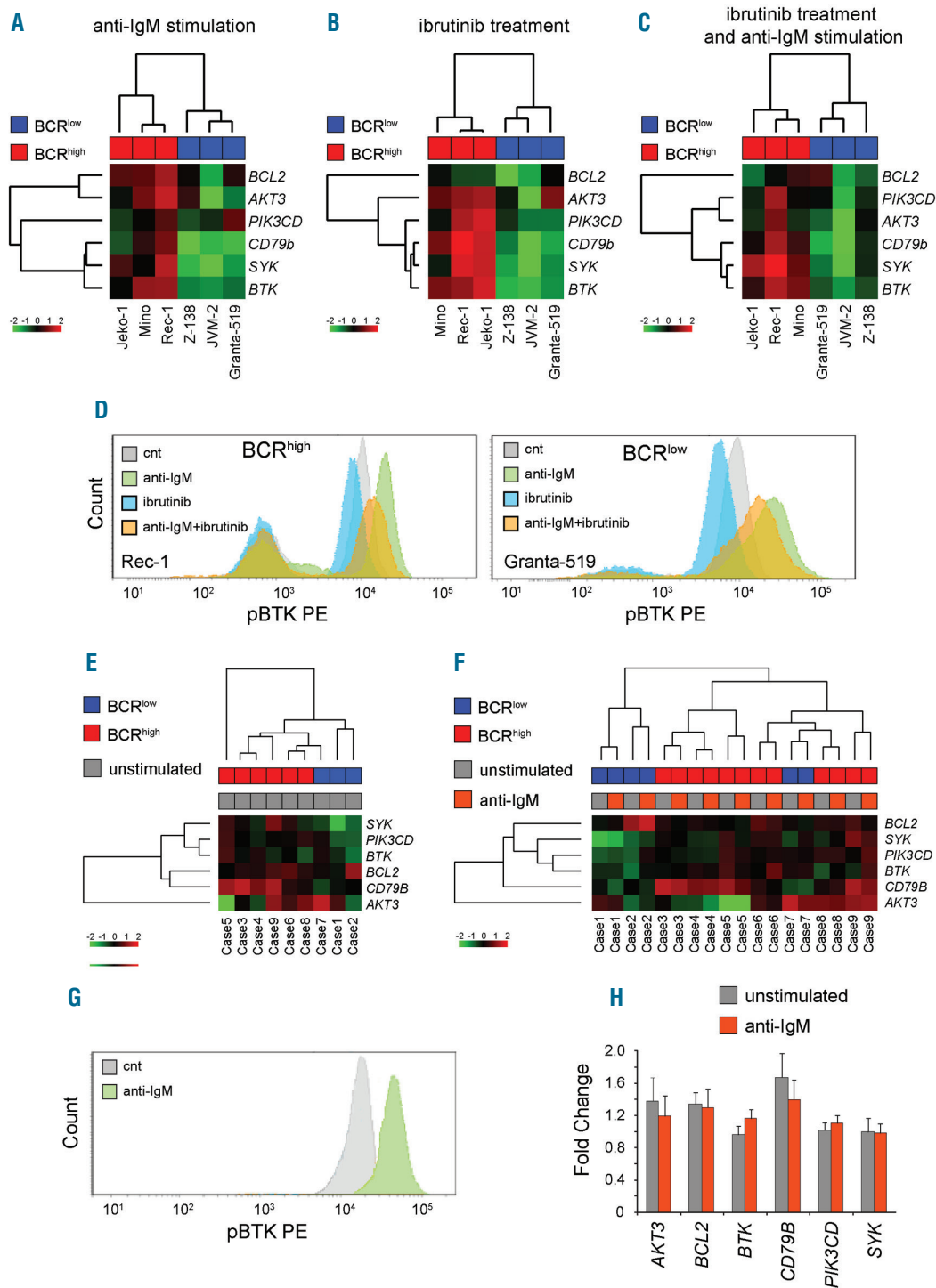


**Figure 2. Anti-IgM stimulation and ibrutinib treatment.** (A) Quantitative real-time polymerase chain reaction (qRT-PCR) analysis of 6-gene signature in mantle cell lymphoma (MCL) cell lines upon soluble anti-IgM stimulation. Hierarchical clustering of three BCR<sup>low</sup> MCL cell lines (blue bar under the horizontal dendrogram) and three BCR<sup>high</sup> MCL cell lines (red bar under the horizontal dendrogram) is shown. (B) qRT-PCR analysis of 6-gene signature in MCL cell lines upon ibrutinib treatment. Hierarchical clustering of three BCR<sup>low</sup> MCL cell lines (blue bar under the horizontal dendrogram) and three BCR<sup>high</sup> MCL cell lines (red bar under the horizontal dendrogram) is shown. (C) qRT-PCR analysis of 6-gene signature in MCL cell lines upon soluble anti-IgM stimulation and ibrutinib treatment. Hierarchical clustering of three BCR<sup>low</sup> MCL cell lines (blue bar under the horizontal dendrogram) and three BCR<sup>high</sup> MCL cell lines (red bar under the horizontal dendrogram) is shown. (D) The histogram plot overlays show (p)-BTK in unstimulated, anti-IgM stimulated, ibrutinib treated and anti-IgM+ibrutinib treated cells from one representative BCR<sup>high</sup> (Rec-1), and BCR<sup>low</sup> (Granta-519) MCL cell lines. (E) qRT-PCR analysis of 6-gene signature in unstimulated MCL primary samples. Hierarchical clustering of three BCR<sup>low</sup> MCL samples (blue bar under the horizontal dendrogram) and six BCR<sup>high</sup> MCL samples (red bar under the horizontal dendrogram) is shown. (F) qRT-PCR analysis of 6-gene signature in MCL primary samples upon anti-IgM stimulation. Hierarchical clustering of three BCR<sup>low</sup> MCL samples (blue bar under the horizontal dendrogram) and six BCR<sup>high</sup> MCL samples (red bar under the horizontal dendrogram) is shown. (G) Phospho-flow analysis of (p)-BTK. The histogram plot overlays show (p)-BTK in unstimulated, and anti-IgM stimulated cells from one representative MCL case. (H) Bar chart plot of qRT-PCR values in nine MCL primary samples upon anti-IgM stimulation. Data represent mean±Standard Error of Mean. P-values refer to paired Student t-test. Color codes for gene expression values refer to mean centered log-ratio values.

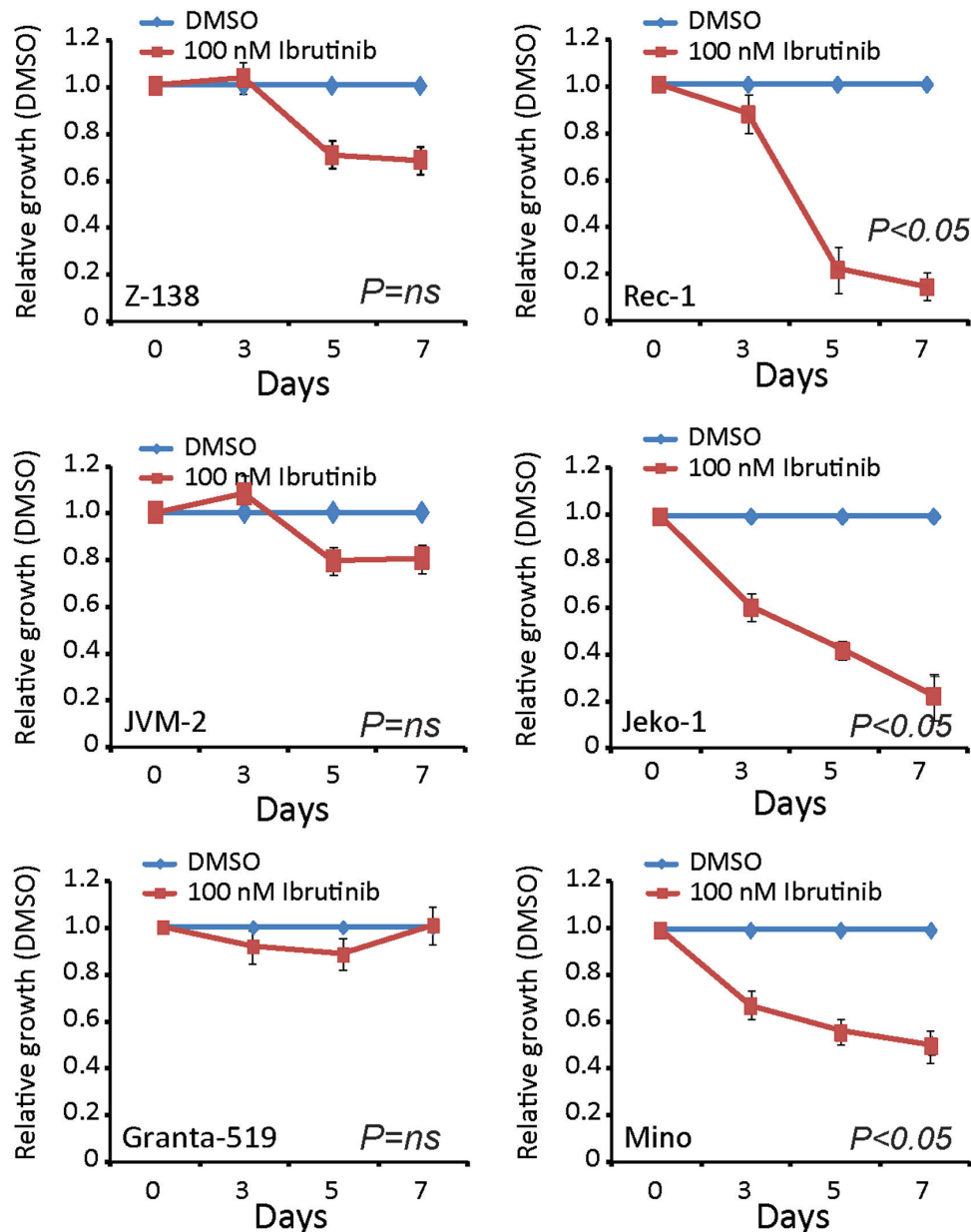


**Figure 3. Mantle cell lymphoma (MCL) cell lines and ibrutinib sensitivity.** Sensitivity of different MCL cell lines to ibrutinib treatment. MCL cell lines were treated with dimethyl sulfoxide (DMSO) (blue line) or ibrutinib (red line). At the indicated time, the number of viable cell/mL was measured with a trypan blue exclusion assay. Z-138, JVM-2, Granta-519 were considered insensitive to ibrutinib treatment while Rec-1, Mino, and Jeko-1 were considered to be highly sensitive. Data represent mean  $\pm$  Standard Error of Mean. *P*-values refer to one sample *t*-test. ns: not significant.

the six genes, thus recapitulating in these cell lines the original observation made in primary MCL samples (Figure 1A).<sup>7</sup> By applying the same decision tree (DT) model previously developed for primary MCL patients,<sup>7</sup> the cell lines JVM-2, Granta-519, and Z-138, all with low expression of the 6-gene signature, were classified as BCR<sup>low</sup>, while the other three cell lines, Rec-1, Jeko-1, Mino, characterized by higher expression levels of the 6-gene signature, were classified as BCR<sup>high</sup>, in agreement with the hierarchical cluster result (Figure 1A).

To confirm the prediction of the BCR status, as determined by the application of the DT model, a wider analysis using a global gene expression profiling (GEP)

approach was performed on the same MCL cell lines (further details in the *Online Supplementary Methods*). Supervised analysis, according to the BCR classification defined by the DT models, discovered a gene expression signature composed of 2,127 probes, 1,183 up-regulated and 944 down-regulated in BCR<sup>low</sup> versus BCR<sup>high</sup> MCL cell lines (*Online Supplementary Table S1*). A hierarchical cluster, generated using the differentially expressed probes, was able to correctly split BCR<sup>low</sup> MCL cell lines from BCR<sup>high</sup> MCL cell lines (Figure 1B). Gene set enrichment analysis (GSEA) highlighted a constitutive overexpression of genes related to the BCR signaling pathways in the context of BCR<sup>high</sup> MCL cell lines (Figure 1C), again con-

firming the results obtained by the DT model. We identified the presence of *TP53* mutations in 4 of 6 cell lines (3 BCR<sup>high</sup> and 1 BCR<sup>low</sup>), suggesting that BCR classification was not related to *TP53* mutational status (Online Supplementary Table S2). These data are in keeping with findings of the original manuscript<sup>7</sup> where, also in the context of primary MCL samples, no correlation between BCR classification and *TP53* mutational status was demonstrated (*data not shown*). On the contrary, while there was no differential expression of *SOX11* between the BCR<sup>high</sup> and BCR<sup>low</sup> primary MCL samples used in our previous paper,<sup>7</sup> in the context of MCL cell line models, a significant upregulation of *SOX11* in BCR<sup>high</sup> cell lines was observed (Online Supplementary Table S1).

Since the 6-gene signature is related to genes involved in the BCR engagement, we evaluated the mRNA expression level changes for these genes in time course experiments at 1 hour (h), 6 h, and 24 h in MCL cell lines after either stimulation of the BCR by anti-IgM (10 µg/mL), or inhibition of the BCR pathway by ibrutinib treatment (100 nM), or a combination of both these approaches (further details in the Online Supplementary Methods). After 24 h of stimulus, hierarchical clusters using the qRT-PCR values of the 6-gene signature clearly differentiated between BCR<sup>high</sup> and BCR<sup>low</sup> MCL cell lines (Figure 2A-C), indicating that the expression of these genes represented an inherent feature of the different cell lines not influenced by anti-IgM and/or ibrutinib treatment, which in turn, as expected, modulated BTK phosphorylation (Figure 2D).<sup>9</sup> The same results were obtained using the earlier (1 h and 6 h) time points (*data not shown*). In order to verify whether this phenomenon remained true also in MCL cells from primary MCL samples, purified MCL cells from nine samples (3 BCR<sup>low</sup> and 6 BCR<sup>high</sup>, accordingly to the DT prediction model) were stimulated for 24 h with anti-IgM. Again, a hierarchical clustering indicated that the 6-gene signature remained stable upon anti-IgM stimulation (Figure 2D and E), although inducing the expected BTK phosphorylation (Figure 2G).<sup>9</sup> In agreement with these data, no significant differences were found between unstimulated and stimulated values according to Student paired *t*-test (Figure 2H), again indicating that the mRNA expression levels of the gene of the 6-gene signature were not influenced by external stimuli such as BCR engagement.

Previous reports demonstrated that the BTK inhibitor ibrutinib displayed highly selective activity in a subset of MCL cell lines.<sup>8,10</sup> Starting from this observation, we tested the capability of ibrutinib treatment (100 nM for 7 days) to impair the proliferation of MCL cell lines. A different response pattern to that seen with ibrutinib treatment was observed (Figure 3). In particular, in agreement with previous reports,<sup>8,10</sup> JVM-2, Granta-519, and Z-138 cell lines were insensitive to ibrutinib treatment while the Rec-1, and Jeko-1 were seen to be sensitive, and Mino had an 'intermediate' sensitivity to ibrutinib treatment, showing approximately 50% cell survival at day 7.

By combining data related to ibrutinib sensitivity and BCR signature, it was seen that sensitive cell lines (Rec-1, Jeko-1 and Mino) were those showing higher expression levels of genes from the 6-gene signature and thus classified as BCR<sup>high</sup> (Figure 1A), while insensitive cell lines (JVM-2, Granta-519, and Z-138), by expressing lower levels of the 6-gene signature, were classified as BCR<sup>low</sup>. We then tested the correlation of BCR signature and ibrutinib sensitivity also in six primary MCL samples (3 BCR<sup>high</sup> and 3 BCR<sup>low</sup>) (Online Supplementary Figure S1A) with available PB viable cells. In keeping with the results reported for MCL cell lines models, BCR<sup>high</sup> cases dis-

played a significant higher sensitivity to ibrutinib treatment with respect to BCR<sup>low</sup> samples (Online Supplementary Figure S1B). When analyzed for the capacity of response to anti-IgM stimulation in terms of BTK phosphorylation, BCR<sup>high</sup> cases showed greater BTK phosphorylation with respect to BCR<sup>low</sup> cases after anti-IgM stimulation (Online Supplementary Figure S1C). These data underline the possibility that BCR<sup>high</sup> samples are more addicted to BCR stimulation and for this reason more sensitive to ibrutinib treatment. Further studies are needed, either on cell lines or on primary MCL cells, to precisely evaluate the discriminative capacity of the proposed classification method, and/or to alternatively test the 6-gene signature using approaches of direct amplification-free RNA quantification.

Despite high response rates and an improvement in PFS, current front-line approaches will inevitably fail and patients will relapse. Moreover, since the treatment choice at relapse depends on many different factors, in the era of new BCR inhibitors, one of the preferred approved therapies includes combination regimens containing the BTK inhibitor ibrutinib, both in the front-line and relapse settings.<sup>3</sup> Despite the relatively high response rate to single agent ibrutinib in MCL, some patients show clear responses, while others obtained a modest therapeutic benefit.<sup>11-13</sup>

Our data underline the clinical significance of the BCR-related genes in the context of drugs specifically targeting genes belonging to this pathway. In fact, through the application of the proposed 6-gene signature, we were able to identify a MCL subset of cases (labeled as being BCR<sup>high</sup>) that appeared more addicted to BCR stimulation with respect to MCL cases with BCR<sup>low</sup> profile, thus explaining the diverse responses of MCL patients to ibrutinib, together with other recently reported causes of primary resistance.<sup>8,14</sup>

In conclusion, this newly developed and validated signature, as well as predicting poor response in the context of a high-dose chemo-immunotherapy regimen, is associated with an increased sensitivity of MCL cell lines to BTK inhibitor exposure. In this regard, given the wider use of ibrutinib in MCL as first-line at relapse, this signature could be included and analyzed together with other recent gene expression-based assays of clinical utility for MCL<sup>15</sup> in future research into risk-adapted therapeutic strategies in trials testing the new BCR inhibitor molecules.

Tiziana D'Agaro,<sup>1</sup> Antonella Zucchetto,<sup>1</sup> Filippo Vit,<sup>1,2</sup> Tamara Bittolo,<sup>1</sup> Erika Tissino,<sup>1</sup> Francesca Maria Rossi,<sup>1</sup> Massimo Degan,<sup>1</sup> Francesco Zaja,<sup>3</sup> Pietro Bulian,<sup>1</sup> Michele Dal Bo,<sup>1</sup> Simone Ferrero,<sup>4,5</sup> Marco Ladetto,<sup>4,6</sup> Alberto Zamò,<sup>7</sup> Valter Gattei<sup>1</sup> and Riccardo Bomben<sup>1</sup>

VG and RB equally contributed to this work as senior authors

<sup>1</sup>Clinical and Experimental Onco-Hematology Unit, Centro di Riferimento Oncologico di Aviano (CRO), IRCCS, Aviano; <sup>2</sup>Department of Life Science, University of Trieste, Trieste; <sup>3</sup>Department of Internal Medicine and Haematology, Maggiore General Hospital, University of Trieste, Trieste; <sup>4</sup>Department of Molecular Biotechnologies and Health Sciences, Hematology Division 1, University of Torino, Torino; <sup>5</sup>Hematology Division 1, AOU "Città della Salute e della Scienza di Torino" University-Hospital, Torino; <sup>6</sup>SC Ematologia Azienda Ospedaliera Nazionale SS. Antonio e Biagio e Cesare Arrigo, Alessandria and <sup>7</sup>Department of Oncology, University of Torino, Torino, Italy

Funding: the authors would like to thank Progetto Giovani Ricercatori GR-2011-02347441, GR-2011-02351370, and GR-



2011-02346826, Ministero della Salute, Rome, Italy; Progetto Ricerca Finalizzata PE 2016-02362756, Ministero della Salute, Rome, Italy; Associazione Italiana Ricerca Cancro (AIRC), Investigator Grant IG-2018 (21687); Associazione Italiana contro le Leucemie, linfomi e mielomi (AIL), Venezia Section, Pramaggiore Group, Italy; Linfo-check - Bando ricerca - contributo art. 15, comma 2, lett b) LR 17/2014; "5x1000 Intramural Program", Centro di Riferimento Oncologico, Aviano, Italy.

Correspondence: RICCARDO BOMBEN - rbomben@cro.it  
doi:10.3324/haematol.2018.212811

Information on authorship, contributions, and financial & other disclosures was provided by the authors and is available with the online version of this article at [www.haematologica.org](http://www.haematologica.org).

## References

- Dreyling M, Ferrero S, Vogt N, Klapper W. New paradigms in mantle cell lymphoma: is it time to risk-stratify treatment based on the proliferative signature? *Clin Cancer Res*. 2014;20(20):5194-5206.
- Ghielmini M, Zucca E. How I treat mantle cell lymphoma. *Blood*. 2009;114(8):1469-1476.
- Cheah CY, Seymour JF, Wang ML. Mantle Cell Lymphoma. *J Clin Oncol*. 2016;34(11):1256-1269.
- Herrmann A, Hoster E, Zwingers T, et al. Improvement of overall survival in advanced stage mantle cell lymphoma. *J Clin Oncol*. 2009;27(4):511-518.
- Barista I, Romaguera JE, Cabanillas F. Mantle-cell lymphoma. *Lancet Oncol*. 2001;2(3):141-148.
- Martin P, Chadburn A, Christos P, et al. Outcome of deferred initial therapy in mantle-cell lymphoma. *J Clin Oncol*. 2009;27(8):1209-1213.
- Bomben R, Ferrero S, D'Agaro T, et al. A B-cell receptor-related gene signature predicts survival in mantle cell lymphoma: results from the Fondazione Italiana Linfomi MCL-0208 trial. *Haematologica*. 2018;103(5):849-856.
- Rahal R, Frick M, Romero R, et al. Pharmacological and genomic profiling identifies NF-kappaB-targeted treatment strategies for mantle cell lymphoma. *Nat Med*. 2014;20(1):87-92.
- Woyach JA, Furman RR, Liu TM, et al. Resistance mechanisms for the Bruton's tyrosine kinase inhibitor ibrutinib. *N Engl J Med*. 2014;370(24):2286-2294.
- Ma J, Lu P, Guo A, et al. Characterization of ibrutinib-sensitive and -resistant mantle lymphoma cells. *Br J Haematol*. 2014;166(6):849-861.
- Wang ML, Rule S, Martin P, et al. Targeting BTK with ibrutinib in relapsed or refractory mantle-cell lymphoma. *N Engl J Med*. 2013;369(6):507-516.
- Wang ML, Blum KA, Martin P, et al. Long-term follow-up of MCL patients treated with single-agent ibrutinib: updated safety and efficacy results. *Blood*. 2015;126(6):739-745.
- Maddocks K. Update on Mantle Cell Lymphoma. *Blood*. 2018;132(16):1647-1656.
- Lenz G, Balasubramanian S, Goldberg J, et al. Sequence variants in patients with primary and acquired resistance to ibrutinib in the phase 3 MCL3001 (RAY) trial. *Haematologica*. 2016;101(s1):155.
- Scott DW, Abrisqueta P, Wright GW, et al. New Molecular Assay for the Proliferation Signature in Mantle Cell Lymphoma Applicable to Formalin-Fixed Paraffin-Embedded Biopsies. *J Clin Oncol*. 2017;35(15):1668-1677.